Science Signaling
AAAS

www.sciencesignaling.org/cgi/content/full/2/61/ra10/DC1

Supplementary Materials for

Rac1 Is a Critical Mediator of Endothelium-Derived Neurotrophic Activity

Naoki Sawada, Hyung-Hwan Kim, Michael A. Moskowitz, James K. Liao*

*To whom correspondence should be addressed. E-mail: jliao@rics.bwh.harvard.edu

Published 10 March 2009, *Sci. Signal.* **2**, ra10 (2009)
DOI: 10.1126/scisignal.2000162

This PDF file includes:

Materials and Methods

Supplementary Text
Fig. S1. CD31 labeling of $Rac1^{+/-}$ and $Rac1^{+/+}$ ECs.
Fig. S2. $Rac1^{+/-}$ ECs show retarded proliferation, migration, and capillary formation.
Fig. S3. CD31 labeling of MBECs.
Table S1. Representative gene sets enriched in $Rac1^{+/+}$ mouse ECs.
Table S2. Representative gene sets enriched in $Rac1^{+/-}$ mouse ECs.
Table S3. Transcription factors differentially expressed between $Rac1^{+/-}$ and $Rac1^{+/+}$ mouse ECs.
Table S4. List of differentially expressed genes between $Rac1^{+/-}$ and $Rac1^{+/+}$ mouse ECs.

Supplementary material
Supplementary Materials and Methods

Generation of EC-*Rac1*$^{+/-}$ mice.
All experimental procedures on animals were performed by using protocols approved by the Harvard Medical School's Standing Committee on Animal Welfare and Protection and are in accordance with the Guide for the Care and Use of Laboratory Animals, published by NIH. Mice were bred and maintained with a 12/12-hour light/dark cycle and fed standard chow with tap water available ad libitum. Age-matched male littermates (12–20 wk) were used for test and control groups in all experiments. *Rac1* conditional allele knock-in mice were developed as described (*1*), and backcrossed at least eight times onto the C57BL/6 strain. Tie2-Cre transgenic mice were obtained from Jackson Laboratory and maintained on C57BL/6 background (*2*) . *Rac1*$^{flox/flox}$ mice were crossed with Tie2-Cre Tg mice to generate EC-*Rac1*$^{+/-}$ (Tie2-Cre *Rac1*$^{flox/+}$) and control (*Rac1*$^{flox/+}$) mice. For some experiments, global *Rac1* haploinsufficient (*Rac1*$^{+/-}$) and control (*Rac1*$^{+/+}$) mice were also used (*1*). The genotyping PCR primers for *Rac1* conditional and null alleles are described previously (*1*). The genotyping primers used for Tie2-Cre transgenic mice are: 5'-TGA TGA GGT TCG CAA GAA CC; 5'-ACC AGT TTA GTT ACC CCC AG.

Transient middle cerebral artery occlusion model.
Mice were anesthetized with 2% isoflurane mixed in 70% N_2O and 30% O_2, and then maintained on 1.5% to 2% isoflurane in a similar gaseous mixture. Transient focal cerebral ischemia was performed using an 8-0 nylon monofilament coated with silicone, which was introduced into the internal carotid artery via the external carotid artery, and then advanced 10 mm distal to the carotid bifurcation to occlude the MCA as described (*3*). Laser Doppler flowmetry of relative CBF was used to verify successful occlusion (<20% baseline value). The MCA was occluded 2 hr, followed by withdrawal of filament and reperfusion for 22 hr. Relative CBF returned to >95% of baseline values, indicating almost complete reperfusion without residual occlusion.

Cerebral infarct volume was measured 22 hr after reperfusion. Infarct area was measured in 2-mm-thick coronal brain sections stained with 2,3,5-triphenyltetrazolium chloride and quantitated with MCID Elite M6 image-analysis software (Interfocus Imaging). Cerebral infarct volume was determined by summing up the infarcted areas. The infarct and edema volumes relative to the non-ischemic hemisphere were calculated as follows: Infarct volume (%) = (non-ischemic hemisphere vol. (mm^3) – ischemic hemisphere non-infarcted region vol. (mm^3))/(non-ischemic hemisphere vol. (mm^3)) × 100. Edema volume (%) = (ischemic hemisphere vol. (mm^3) – non-ischemic hemisphere vol. (mm^3))/(non-ischemic hemisphere vol. (mm^3)) × 100.

The neurological deficit score (NDS) was determined at 20 hr post-reperfusion by two observers, who were blinded to the identity of the mice or treatment protocol. The following scoring system was used: 0, no motor deficits (normal); 1, flexion of the contralateral torso and forelimb on lifting the animal by the tail (mild); 2, circling to the contralateral side but normal posture at rest (moderate); 3, leaning to the contralateral side at rest (severe); and 4, no spontaneous movement (critical).

Absolute CBF in ischemic and non-ischemic hemispheres was measured at the end of 2 hr MCAo using an indicator fractionation technique as described, with slight modifications (*3*). Briefly, the right jugular vein and left femoral artery of anesthetized mice were cannulated. The mice received 1 μCi of N-isopropyl-[methyl 1,3-^{14}C] p-iodoamphetamine from the right jugular vein as a bolus. A volume of 100 μL of arterial blood samples from the left femoral artery was collected for 20 sec (0.3 ml/min), and then the animal was decapitated and the whole brain was removed. The brain was immediately cut into the 2 hemispheres and frozen in chilled isopentane solution chilled with dry ice immediately. The frozen hemispheres were weighed and digested with Scintigest (Fischer Scientific) at 50°C for 6 h. Scintillation fluid and H_2O_2 were added to the sample and they were shaken together for 12 h. The radioactivity in the blood and brain samples was measured by liquid scintillation spectrometry (RackBeta 1209). Cerebral blood flow in each hemisphere was calculated as follows: CBF (ml/100 g per min) = (hemisphere count (c.p.m.) × 0.3 (ml/min))/(blood count (c.p.m.) × hemisphere weight (g)) × 100. The relative CBF change in ischemic hemisphere was determined as: CBF change (%) = (ischemic hemisphere CBF (ml/100 g per min) – non-ischemic hemisphere CBF (ml/100 g per min))/(non-ischemic hemisphere CBF (ml/100 g per min)) × 100.

Isolation and culture of mouse primary ECs.
Mouse primary ECs were isolated from the heart by an affinity selection method using Dynabeads sheep anti-rat IgG (Invitrogen) and anti-PECAM1 antibody (BD Biosciences) as described (*4*). The cells were cultivated in DMEM containing 20% FCS, heparin (100 μg/ml), penicillin (100 U/ml), streptomycin (100 μg/ml) and endothelial cell growth factor (ECGF, 50 μg/ml), and grown on dishes coated with 0.1% gelatin. After 8 days, the cells were trypsinized and underwent the second selection using Dynabeads plus anti-ICAM2 antibody (BD Biosciences). Mouse ECs were used for experiments at passage 3-5.

GTP-Rac1 pull down assay and immunoblotting analysis.
pGEX-2T-PAK-CRIB domain construct is a gift from Dr. John G. Collard. Preparation of GST-PAK-CD and GTP-Rac1 pull down assay was performed as described (*5*). The GTP-Rac1, total Rac1 and actin protein levels in mouse EC lysate were determined by immunoblotting analysis with Rac1 (BD Biosciences) and actin (Sigma) antibodies. The blots were subsequently probed with HRP-conjugated secondary antibody and visualized by Enhanced Chemiluminescence (GE Health Care).

Microarray expression profiling.
Rac1$^{+/-}$ and *Rac1*$^{+/+}$ mouse primary ECs were isolated from 6 mice/genotype derived from 2 age-matched litters (12 wk). Following the first and the second sorting, subconfluent ECs at passage 4 were used for the isolation of RNA. To validate the purity of the EC population, a portion of the cells was immunolabeled with FITC-conjugated anti-mouse CD31 antibody (eBioscience). Flow cytometric analysis revealed that > 98% of the *Rac1*$^{+/-}$ and *Rac1*$^{+/+}$ ECs were positive for CD31 (fig. S1). High quality total RNA was prepared by 2-step purification through the sequential use of Trizol reagent (Invitrogen) and RNeasy columns (Qiagen) according to the manufacturer's instructions. The quality control of RNA was conducted by measuring the 28S/18S rRNA ratio using Agilent 2100 BioAnalyzer. cDNA labeling, hybridization and image acquisition was performed at Massachusetts General Hospital Microarray Core. Briefly, fluorescent dye labeling was performed using the Atlas Powerscript Fluorescent Labeling Kit (Clontech). Isolated total RNA (8 μg) was reverse transcribed into amine modified cDNA using random hexamers and oligo (dT) primers in 4 replicates per each genotype. The cDNA was labeled via a coupling reaction to the Cy3 (2 replicates) or Cy5 (2 replicates) dye, then purified and concentrated. Equimolar mixtures of Cy3-labeled *Rac1*$^{+/+}$ and Cy5-labeled *Rac1*$^{+/-}$ probes (or dye-swapped combinations) were independently hybridized to 4 microarray slides. The microarray was a glass-based pre-printed array containing PGA Mouse v1.1 probe set (19,549 70-mer oligonucleotides), which provides complete coverage of the 2002 Mouse genome, built off the GenPept database. Images were acquired using Axon (Molecular Devices) 4000B 2-color single-slide scanner. Filtering, normalization of the raw data and basic statistical tests were conducted using BASE software. All spots were sequentially subjected to background subtraction, Lowess normalization, and brightness filtering that removed spots with intensities less than 200. This processing resulted in 12,089 reporters (gene features) comprising 45,311 spots from the 4 slides. The averaged fold ratio of *Rac1*$^{+/-}$ versus *Rac1*$^{+/+}$ was calculated for each reporter and statistically analyzed using 1 sample Student t-test and Wilcoxon signed rank test, yielding 1,431 reporters considered significant at a confidence level of 95% ($P < 0.05$). The averaged fold ratios distributed with 2 SD of 1.56. Gene reporters with the fold ratio of > 1.5 or < –1.5 were considered differentially expressed between *Rac1*$^{+/+}$ and *Rac1*$^{+/-}$ ECs.

Gene cluster and pathway analysis.
To characterize the enrichment profiles of gene clusters and pathways in *Rac1*$^{+/-}$ and *Rac1*$^{+/+}$ ECs, we conducted 2 different analyses.
<u>DAVID Functional Annotation Clustering (*6*).</u>
The 138 upregulated (fold ratio > 1.5) and 161 downregulated (fold ratio < –1.5) reporters were imported into DAVID 2007 software (http://david.abcc.ncifcrf.gov/home.jsp) and collapsed to 130 and 138 unique genes, respectively, using the DAVID accession conversion tool. The upregulated and downregulated gene lists were separately uploaded for gene annotation analysis. Enrichment of a given gene annotation in each gene list against the default Mus Musculus background was determined by EASE score, a modified Fisher Exact *P*-Value. The DAVID default setting was used for the source databases of gene

annotation: Gene Ontology (GOTERM_BP_ALL, GOTERM_CC_ALL, GOTERM_MF_ALL), Protein Domains (INTERPRO, PIR_SUPERFAMILY, SMART), Pathways (BIOCARTA, KEGG_PATHWAY), and Functional Categories (COG_ONTOLOGY, SP_PIR_KEYWORDS, UP_SEQ_FEATURE). Subsequently, Functional Annotation Clustering was performed to measure relationships among the annotation terms based on the degrees of their co-association genes to group the similar, redundant, and heterogenous contents from the same or different resources into annotation groups. The Functional Annotation Clustering integrates Kappa statistics to measure the common genes between two annotations, and fuzzy heuristic clustering to classify the groups of similar annotations according to kappa values. The biological significance of functional annotation clusters was ranked by the Enrichment Score, which is the geometric mean (in –log scale) of member's EASE scores within each cluster.

Gene Set Enrichment Analysis (GSEA) (*7*).

To test for sets of related genes that might be systematically altered in *Rac1*$^{+/-}$ ECs, we used Gene Set Enrichment Analysis (GSEA), a method that combines information from members of previously defined sets of genes to increase signal relative to noise and improve statistical power to detect subtle changes. Complete details on the method for this analysis, the software and information on the biological data sets are available at http://www.broad.mit.edu/gsea/index.jsp. Briefly, genes from the microarray were first ranked according to the expression difference (signal to noise ratio) between *Rac1*$^{+/-}$ and *Rac1*$^{+/+}$ ECs. The standard GSEA null hypothesis is that the rank ordering of the genes in a given comparison is random and not associated with the order of the genes and/or treatment. The extent of association was then measured by a non-parametric running sum statistic termed the enrichment score (ES), and the maximum ES (MES) was recorded over each gene set. Phenotype permutation testing was used to assess the statistical significance of the MES, which was calculated as the fraction of 1,000 random permutations of the gene list. The unadjusted nominal *P* value estimated the statistical significance of a gene set without adjusting for gene set size or multiple hypothesis testing, whereas the false discovery rate (FDR) statistic adjusts for both. In the present study, we used curated gene sets (C2), archived at Molecular Signature Database, which were collected from various sources such as online pathway databases, publications in PubMed, and knowledge of domain experts. Among these gene sets, 1782 sets with the gene set size > 15 were used for analysis, and 161 gene sets were significantly upregulated in *Rac1*$^{+/-}$, whereas 145 sets were enriched in *Rac1*$^{+/+}$ ECs at FDR < 25%.

Quantitative RT-PCR.

Total RNA was extracted from the mice brains and ECs using RNeasy mini kit (Qiagen) with DNase I treatment, and 50-100 ng of total RNA was used for one-step real-time RT-PCR using QuantiTect SYBR Green RT-PCR kit (Qiagen) according to the manufacturer's instruction. The reaction was performed with 7900HT Fast Real-Time PCR System (Applied Biosystems). The mRNA level was normalized with that of either GAPDH mRNA or 18S rRNA. The PCR primers used are: Rac1, 5'-GAG ACG GAG CTG TTG GTA AAA, 5'- ATA GGC CCA GAT TCA CTG GTT; Artemin, 5'-CCC TAG CTG TTC TAG CCC TG, 5'-AGG GTT CTT TCG CTG CAC AA; FGF5, 5'-AAG TAG CGC GAC GTT TTC TTC, 5'- CTG GAA ACT GCT ATG TTC CGA G; BMP6, 5'-AGA AGC GGG AGA TGC AAA AGG, 5'-GAC AGG GCG TTG TAG AGA TCC; TGFα, 5'-CAC TCT GGG TAC GTG GGT G, 5'-CAC AGG TGA TAA TGA GGA CAG C; Crystallin αB, 5'-GTT CTT CGG AGA GCA CCT GTT, 5'-GAG AGT CCG GTG TCA ATC CAG; VCAM-1, 5'-AGT TGG GGA TTC GGT TGT TCT, 5'-CCC CTC ATT CCT TAC CAC CC; Gpx3, 5'-CCT TTT AAG CAG TAT GCA GGC A, 5'-CAA GCC AAA TGG CCC AAG TT; Thrombospondin 2, 5'-CTG GGC ATA GGG CCA AGA G, 5'-GCT TGA CAA TCC TGT TGA GAT CA; GAPDH, 5'-AGG TCG GTG TGA ACG GAT TTG, 5'-TGT AGA CCA TGT AGT TGA GGT CA; 18S, 5'-AAA TCA GTT ATG GTT CCT TTG GTC, 5'-GCT CTA GAA TTA CCA CAG TTA TCC AA.

Immunofluorescence staining.

Mouse ECs were cultured to subconfluence on Labtek II chamber slides (Nunc) under standard culture conditions. Cells were fixed with 3.7% paraformaldehyde in PBS for 10 min on ice, and then free aldehyde was reduced with 50 mM NH_4Cl. The cells were subsequently permeabilized with 0.1% Triton X-100 in PBS for 5 min, and blocked with 1% BSA in PBS for 30 min at room temperature. For F-actin staining, the cells were incubated with 1U/ml Alexa488-conjugated phalloidin (Molecular Probe) for 20 min. For immunostaining, the cells were incubated with rabbit anti-ß tubulin (Lab Vision) or mouse anti-

crystallin αB antibody (Stressgen) at 4˚C overnight. After wash, the cells were labeled with the corresponding secondary antibody conjugated with Alexa488 (Molecular Probe) for 1 hr at room temperature. The fluorescent images were acquired by TCS SP5 confocal microscope (Leica). F-actin and ßtubulin fluorescence was quantified with Photoshop and Image J softwares.

Hypoxia treatment.
Cells were placed without culture dish covers in humidified airtight chambers (Billups-Rothenberg) perfused with 95% N_2 and 5% CO_2 at 2 psi for 10 min. The chambers were sealed and maintained at 37˚C for indicated time periods. At the end of hypoxia exposure, cells were removed from the chamber and returned to a regular incubator for reoxygenation. Control cultures were incubated in a regular incubator under normoxic condition for the corresponding hypoxic duration.

Assessment of NADPH oxidase activity.
Mouse ECs were grown to confluence on 96-well plates. The cells were treated without or with 10 μM Diphenyleneiodonium chloride (DPI), a NADPH oxidase inhibitor, and then exposed to 4-hr hypoxia and 2-hr reoxygenation. The cells were sequentially pre-equilibrated with Hanks' Balanced Salt Solution (HBSS) containing 10 mM Sodium diethyldithiocarbamate trihydrate (DETC) and 1 mM DTT for 30 min, and then with 3.3 μM lucigenin for 5 min. The cells were treated with 67 μM NADPH, and the chemiluminescence was captured for 1 min with a luminometer (Victor3, PerkinElmer). The NADPH oxidase activity was determined as DPI-inhibitable lucigenin chemiluminescence.

Assessment of oxidative stress.
Mouse ECs were grown to confluence on 96-well plates. The cells were loaded with 100 μM 2',7'-dichlorofluorescein diacetate (DCFH-DA) in Krebs-Ringer-HEPES (KRH) buffer, pH 7.4, containing 4% bovine serum albumin and 0.55 mM glucose for 30 min. After the loading buffer was removed, the cells in KRH buffer were exposed to 4-hr hypoxia and 2-hr reoxygenation. The fluorescence caused by oxidation of DCFH-DA to DCF was measured in a plate reader by 485-nm excitation and 530-nm emission filters.

Annexin V binding assay.
Following various apoptosis-inducing conditions, 1-5 $\times$ 10^5 cells were detached with trypsin/EDTA and washed with Annexin V binding buffer (10 mM HEPES, pH 7.4, 140 mM NaCl, 2.5 mM $CaCl_2$). The cells were labeled in 0.2 ml Annexin V binding buffer containing 10 μg/ml Annexin V-EGFP in the dark for 15 min. The cells were pelleted by centrifugation, resuspended in 1 ml binding buffer, and analyzed by flow cytometry with the excitation beam of 488 nm through FL1 detector (Cytomics FC 500, Beckman Coulter). Unstained cells were used as a negative control for background subtraction.

Cell adhesion assay.
Mouse ECs were grown to subconfluence, or kept at confluence for > 4 weeks. Then, the cells were washed 2 times with PBS (Ca^{++}-free), and subjected to standard trypsinization using 0.25% trypsin/1 mM EDTA solution (Invitrogen) at 37˚C. The cells were pipetted and observed under light microscope at the intervals of 3-5 min. The strength of cell adhesion was assessed by the time required for obtaining single cell suspensions (*8*).

Assessment of EC barrier function.
Mouse ECs grown to confluence on Transwell inserts (0.4-μm pore size) were maintained thereafter for ~10 days. The medium in the upper compartment was replaced with fresh medium containing HRP (20 μg/ml), and the cells were exposed to 4-hr hypoxia and 2-hr reoxygenation. Medium from the bottom well was incubated with assay buffer containing 0.5 mM guaiacol, 50 mM Na_2HPO_4 and 0.6 mM H_2O_2. HRP activity was assessed as the formation of *O*-phenylenediamine determined by absorbance at 470 nm (*9*).

Assessment of EC-leucocyte attachment.
Monocyte cell line THP-1 was cultured in RPMI 1640 supplemented with 10% FCS. The THP-1 cells

were labeled with 1 μCi/ml [^{3}H]-thymidine for 48 hr and washed. Confluent mouse ECs in 6-well plates were subjected to 4-hr hypoxia and 20-hr reoxygenation. The ECs were co-cultured with the radiolabelled THP-1 cells (1 million cells per ml) at a static condition for 3 hr. At the end of incubation, non-adherent THP-1 cells were removed and the ECs were washed 3 times with PBS. The remaining adherent cells were lysed with 1mL of 0.5 M NaOH, and the radioactivity was measured in a scintillation counter (*10*).

Isolation and culture of neuronal cells and mouse brain ECs.
The human neuroblastoma cell line SH-SY5Y was purchased from ATCC and maintained in a 1:1 mixture of Eagle's Minimum Essential Medium (EMEM) and F-12 medium, supplemented with 10% FCS and penicillin/streptomycin. Primary cortical neurons were isolated from C57/BL6 fetal mouse brains (~E16). Briefly, dissected cortices were digested with 0.25% trypsin at 37˚C for 10min, and DNase I (25 U/ml) for 5 min. The digested cortices were triturated and passed through a 40-μm strainer. The neurons were plated on cover glasses pre-coated with poly-D-lysine (0.1 mg/ml) at a density of 1-1.5 $\times$ 10^6 cells/well in 6-well plates. The cells were maintained in serum-free Neurobasal medium (Invitrogen) supplemented with 1 mM glutamine, 2% B27 supplement and penicillin/streptomycin, and treated with 25 μg/ml glutamate (day 0-3) and 10 μM Ara-C (day 3-4). Thereafter, half of the medium was replaced with fresh medium every 3 days. The neurons were used for experiments at days 14-21. Mouse brain microvascular endothelial cells (MBEC) were isolated as described with modifications (*11-13*). Age-matched adult EC-Rac1$^{+/-}$ and control mice (n = 6-10 per genotype) from 2-3 litters were used for cell isolation. Dissected cortices were homogenized in ice-cold DMEM/F12 (1:1) using a Dounce tissue grinder (loose pestle) with 5 strokes and further minced by scissors. The homogenate was centrifuged (200 g, 5min, 4˚C), and the pellets were resuspended with 15% dextran (MW ~100,000) in PBS (-) and centrifuged at 10,000 g, 15 min, 4˚C. The pellets were suspended and digested in DMEM/F12 containing Collagenase/Dispase (1mg/ml) (Roche) and DNase I (25 μg/ml) at 37˚C for 90 min, and centrifuged at 400g, 10 min, room temperature. The pellets were suspended with 45% Percoll in PBS, centrifuged at 20,000 g, 15 min, 4˚C. The top layer containing microvessels and ECs were transferred to a new tube, centrifuged at 400 g, and washed once with complete media (DMEM/F12 with 10% horse serum, 10% FCS, heparin, penicillin/streptomycin and ECGF). Cells were plated and grown on gelatin-coated T25 plates, and split at 1:2. More than 95% of MBECs at passage 1 were positive for CD31 staining (fig. S3). MBECs were used for experiments at passage 3-5.

EC-neuron co-culture and assessment of neuronal cell death.
ECs were plated on Transwell culture inserts (0.4-μm pore size) and grown to confluence. ECs and neuronal cells (SH-SY5Y or cortical neurons) were maintained in respective complete media (ECs, upper compartment, 1.5 ml; neuronal cells, lower compartment, 2.6 ml). Following the change of media, co-culture was started by adding inserts with ECs to neuronal cell cultures in 6-well plates. Co-culture proceeded for 48 hr and then the inserts with ECs were removed. SH-SY5Y cells left in the conditioned media were exposed to hypoxic conditions for 24 hr, and the apoptotic cell fraction was assessed through Annexin V-EGFP labeling. Cortical neurons were co-cultured with MBEC in the presence of vehicle, goat anti-mouse artemin neutralizing antibody (0.5 μg/ml), or goat IgG (0.5 μg/ml, R&D) in the lower compartment. Some neurons were treated with blank inserts and recombinant mouse artemin (0–10 ng/ml). The cortical neurons, after co-culture with MBEC, were subjected to oxygen/glucose deprivation (OGD). Briefly, the conditioned media (CM) was removed from the neurons and stored separately. The cells were simultaneously treated with glucose-free DMEM and hypoxia for 2 hr, re-supplied with CM, and returned to normoxic conditions (reoxygenation) for 22 hr. Neurons on cover slips were fixed in 3.7% paraformaldehyde in PBS on ice for 15 min, washed, and permeabilized with methanol at –20˚C for 10 min. The cells were washed, blocked with 1% BSA for 30 min, and probed with cleaved caspase-3 (Asp175) (5A1) rabbit mAb (Cell Signaling) at 4˚C overnight. Following wash, the cells were stained with Alexa568-conjugated anti-rabbit Ab and 4' 6'-diamino-2-phenylindole (DAPI) for 1 hr at room temperature. Images were captured using an epifluorescence microscope. The cleaved caspase 3 positive fraction was analyzed by the Photoshop software.

EC proliferation, migration and capillary formation assays.
For proliferation assay, mouse ECs were plated at ~30% confluency on 24-well plates, and allowed to

grow in complete medium (20% FCS). On day 1 and 3, cells were fixed in neutral buffered 10% formalin for 15 min, washed with water, and stained with 0.1% crystal violet in 200 mM MES (pH6.0) for 1 hr. Following extensive washing with water, plates were dried and cell-associated dye was extracted with 10% acetic acid, and quantitated by absorbance at OD590 (*14*). Cell migration was assessed by scratch assay of the monolayer. Briefly, ECs were grown to confluence, and a linear acellular wound 1.5 mm wide was made with a scraper. The wound edge was marked by a cover slip attached to the bottom of the cultureware. The migrating cells were observed under light microscope and photographed at day 2. The capillary forming capacity of mouse ECs was evaluated in aortic explants *ex vivo*. Aortic segments from mice were embedded in 0.4 ml per well of Matrigel (BD Biosciences) in 24 well plates. After the gel solidified, 0.5 ml of culture media was added and replaced every other day. At day 8, photographs were taken to evaluate capillary outgrowth.

Statistical analysis.

Unless otherwise noted, all statistical analysis was carried out by ANOVA followed by Fisher's test. $P < 0.05$ was considered to be significant.

Supplementary text

Global downregulation of cell cycle-related genes in *Rac1*$^{+/-}$ ECs.

Functional annotation clustering and GSEA revealed that the genes downregulated in *Rac1*$^{+/-}$ are globally associated with mitotic cell division (Fig. 2D, 2F and Tables 2, S1, S3). These included transcription factors (c-fos (*15*), c-myb (*16*), Egr1 (*17*), Runx1 (*18*)), cyclins (cyclin A2, cyclin B2), mitotic kinases (Cdc2, Aurora A (*19*)), regulators of mitotic spindle assembly (Tacc3 (*20*), Tpx2 (*21*), BARD1 (*22*)), mitotic checkpoint (Mad2l1 (*23*), survivin (*24*)), centrosome cycle (Nek2 (*25*)), cytokinesis (Ect2 (*26*)), sister chromatid cohesion (sororin (*27*)), G2/M checkpoint (GADD45γ (*28*)) and cell proliferation index (Ki-67). The downregulated genes further comprised mitotic kinesin-like motor proteins (*29*) associated with spindle assembly (Kif11 (*30*), Kif22 (*31*), Kif23 (*32*)), chromosome alignment (Kif2c (*33*), Kif18a (*34*)) and cytokinesis (Kif20a (*35*)); chromosomal proteins such as linker histone H1, nucleosome histones (H2A, H2B, H3) along with topoisomerase IIα (Top2a). Importantly, many of these genes are induced in a tightly cell cycle-dependent manner (c-myb, Runx1 (*36*), cyclins, Nek2 (*37*), Ect2 (*38*), Aurora A (*39*), Ki-67, histones (*40*), Top2a (*41*)), suggesting that the downregulation of these genes represent overall growth inhibitory state of *Rac1*$^{+/-}$ ECs (fig. S2A). These observations conform well to the previously appreciated roles of Rac1 in critically mediating cell cycle progression (*42-44*), thus confirming the validity of our microarray data.

Anti-angiogenic phenotype of *Rac1*$^{+/-}$ ECs.

The anti-angiogenic phenotype of *Rac1*$^{+/-}$ ECs (fig. S2) is correlated with the growth inhibition and coordinate upregulation of angiostatic genes, Robo4 (*45*), ADAMTS1 (*46*) and thrombospondin 2 (*47*) (Table 3), and consistent with the retardation in ischemia-induced angiogenesis of EC-*Rac1*$^{+/-}$ mice (*48*).

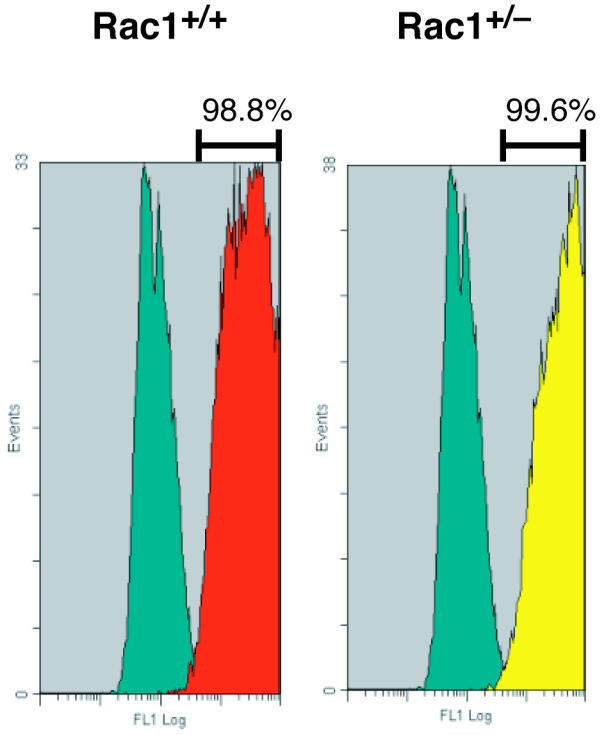

Fig. S1. CD31 labeling of *Rac1*$^{+/-}$ and *Rac1*$^{+/+}$ ECs. *Rac1*$^{+/+}$ and *Rac1*$^{+/-}$ mouse ECs were immunolabeled with anti-CD31 (PECAM1) antibody or control IgG. The fraction of CD31-stained *Rac1*$^{+/+}$ (red) and *Rac1*$^{+/-}$ (yellow) ECs was determined by FACS analysis in comparison to the IgG-stained control ECs (green).

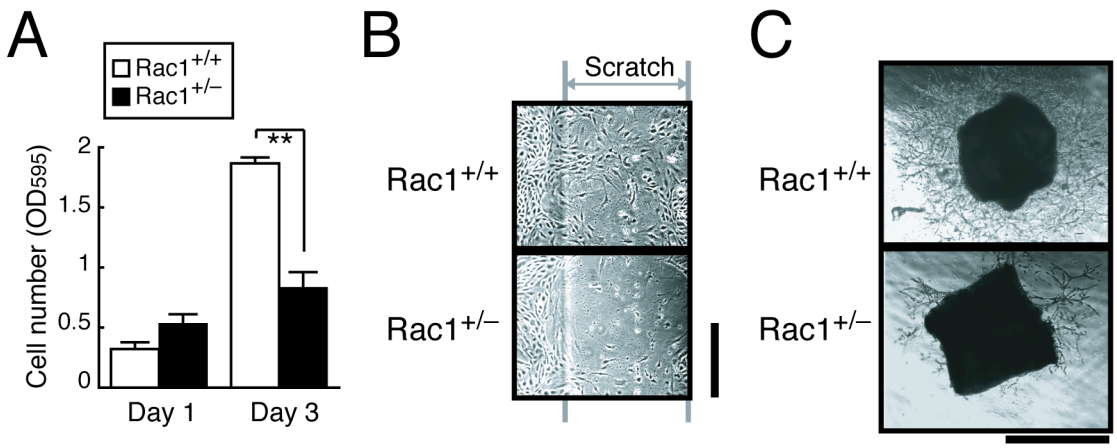

Fig. S2. *Rac1*$^{+/-}$ ECs show retarded proliferation, migration and capillary formation. (**A**) Time-course assessment by crystal violet staining of the cell number of *Rac1*$^{+/+}$ and *Rac1*$^{+/-}$ mouse endothelial cells cultured in the presence of 20% serum. Values are means ± SEM of triplicates (**, $P < 0.01$; ANOVA). (**B**) EC confluent monolayer was scratched at the width of 1.5 mm. Thereafter, the cells were allowed to migrate in the presence of 20% serum. Photographs were taken at 48 hr. Scale bar, 1 mm. (**C**) *Rac1*$^{+/+}$ and *Rac1*$^{+/-}$ mouse aortic segments were embedded in Matrigel, and cultured under the presence of 20% serum to allow for capillary sprouting. Photographs were taken at day 8. Scale bar, 1 mm.

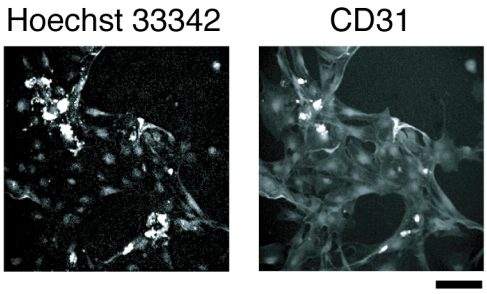

Fig. S3. CD31 labeling of mouse brain ECs (MBECs). MBECs were double stained with Hoechst 33342 (nuclear stain) and anti-CD31 (PECAM1) antibody. CD31 was visualized with Alexa 488-conjugated anti-rat IgG antibody. The fluorescence images were captured with confocal microscope. Scale bar = 50 μm.

Table S1. Representative gene sets enriched in *Rac1*$^{+/+}$ mouse endothelial cells

MSigDB* Gene Set	Brief gene set description	Source publication†	Set Size	ES‡	NES§	NOM p-val¶	FDR q-val‖
GOLDRATH_CELLCYCLE	Cell cycle genes induced during antigen activation of CD8+ T cells.	Goldrath et al. Proc Natl Acad Sci U S A. 2004 101:16885-90.	24	-0.800	-2.183	0	0.015
SERUM_FIBROBLAST_ CELLCYCLE	Cell-cycle dependent genes regulated following exposure to serum in a variety of human fibroblast cell lines	Chang et al. PLoS Biol. 2004 2:E7.	71	-0.760	-2.171	0	0.015
CANCER_ UNDIFFERENTIATED_ META_UP	Sixty-nine genes commonly upregulated in undifferentiated cancer relative to well-differentiated cancer, from a meta-analysis of the OncoMine gene expression database	Rhodes et al. Proc Natl Acad Sci U S A. 2004 101:9309-14.	49	-0.679	-2.145	0	0.016
VANTVEER_BREAST_ OUTCOME_GOOD_VS_ POOR_DN	Poor prognosis marker genes in Breast Cancer (part of NKI-70) from Van't Veer et al 2002	van 't Veer et al. Nature. 2002 415:530-6.	53	-0.626	-2.065	0	0.015
DOX_RESIST_GASTRIC_UP	Upregulated in gastric cancer cell lines reistant to doxorubicin, compared to parent chemosensitive lines	Kang et al. Clin Cancer Res. 2004 10:272-84.	26	-0.865	-2.054	0	0.017
GENOTOXINS_ALL_ 4HRS_REG	Genes regulated in mouse lymphocytes (TK 3.7.2C) at 4 hours by all six genotoxins tested (cisplatin, methyl methanesulfonate, mitomycin C, taxol, hydroxyurea and etoposide)	Hu et al. Mutat Res. 2004 549:5-27.	21	-0.673	-1.914	0.02	0.020
P21_P53_ANY_DN	Down-regulated at any timepoint (4-24 hrs) following ectopic expression of p21 (CDKN1A) in OvCa cells, p53-dependent	Wu et al. J Biol Chem. 2002 277:36329-37.	20	-0.768	-1.896	0	0.022

*Gene sets curated from online pathway databases, publications in PubMed, and knowledge of domain experts are archived at Molecular signatures database (MSigDB) (http://www.broad.mit.edu/gsea) and used for GSEA. †Literature source of the gene set. ‡Enrichment score reflecting the degree to which each gene set is overrepresented at the extreme (*Rac1*$^{+/-}$) of the entire ranked list. §ES normalized to account for the size of the set. ¶Nominal *P* value showing the statistical significance of the ES, which is estimated in 1,000 empirical phenotype-based permutations. ‖False discovery rate showing the proportion of false positives for each NES.

The *Rac1*$^{+/-}$ versus *Rac1*$^{+/+}$ EC datasets were analyzed in GSEA on 1,782 gene sets with minimum set size of 15. Among these, 1,019 gene sets were upregulated in *Rac1*$^{+/-}$ and 763 gene sets were upregulated in *Rac1*$^{+/+}$. Representative gene sets are shown out of 145 gene sets upregulated in *Rac1*$^{+/+}$ with FDR < 0.25.

Table S2. Representative gene sets enriched in *Rac1*$^{+/-}$ mouse endothelial cells

MSigDB Gene Set	Brief gene set description	Source publication	Set Size	ES	NES	NOM p-val	FDR q-val
ADIP_VS_FIBRO_DN	Downregulated following 7-day differentiation of murine 3T3-L1 fibroblasts into adipocytes	Gerhold et al. Endocrinology. 2002 143:2106-18.	21	0.687	1.910	0	0.127
ADIP_VS_PREADIP_DN	Downregulated in mature murine adipocytes (7 day differentiation) vs. preadipocytes (6 hr differentiation)	Gerhold et al. Endocrinology. 2002 143:2106-18.	29	0.615	1.794	0	0.153
MANALO_HYPOXIA_UP	Genes upregulated in human pulmonary endothelial cells under hypoxic conditions or after exposure to AdCA5, an adenovirus carrying constitutively active hypoxia-inducible factor 1 (HIF-1alpha).	Manalo et al. Blood. 2005 105:659-69.	63	0.507	1.785	0	0.143
TGFBETA_ALL_UP	Upregulated by TGF-beta treatment of skin fibroblasts, at any timepoint	Verrecchia et al. J Biol Chem. 2001 276:17058-62.	53	0.570	1.730	0	0.136
HINATA_NFKB_UP	Genes upregulated by NF-kappa B	Hinata et al. Oncogene. 2003 22:1955-64.	55	0.558	1.728	0	0.123
CELL_ADHESION	The attachment of a cell, either to another cell or to the extracellular matrix, via cell adhesion molecules.	curated gene set	92	0.413	1.669	0	0.117
TGFBETA_LATE_UP	Upregulated by TGF-beta treatment of skin fibroblasts only at 1-4 hrs (clusters 4-6)	Verrecchia et al. J Biol Chem. 2001 276:17058-62.	19	0.594	1.656	0.03	0.126

See the footnote for Table S2 for abbreviation.

Representative gene sets are shown out of 161 gene sets upregulated in *Rac1*$^{+/-}$ with FDR < 0.25.

Table S3. Transcription factors differentially expressed between *Rac1*$^{+/-}$ and *Rac1*$^{+/+}$ mouse endothelial cells

Symbol	Gene name	Fold*
Gtf2ird1	general transcription factor II I repeat domain-containing 1	3.01
Med8	mediator of RNA polymerase II transcription, subunit 8 homolog (yeast)	2.62
Zkscan1	zinc finger with KRAB and SCAN domains 1	2.37
Npas3	neuronal PAS domain protein 3 (Npas3)	2.33
Lsr	lipolysis stimulated lipoprotein receptor	2.03
Taf9	TAF9 RNA polymerase II, TATA box binding protein (TBP)-associated factor	1.84
Zfp467	zinc finger protein EZI	1.71
Tle4	transducin-like enhancer of split 4, homolog of Drosophila E(spl)	1.57
Atf5	activating transcription factor 5 (Atf5)	1.50
Pax7	paired box gene 7	–1.55
Myb	myeloblastosis oncogene	–1.57
Zfp69	zinc finger protein 69	–1.71
Runx1	runt related transcription factor 1	–1.73
Foxj2	forkhead box J2	–1.97
Egr1	early growth response 1	–2.46
Fos	FBJ osteosarcoma oncogene	–3.02

* The fold ratio of *Rac1*$^{+/-}$/*Rac1*$^{+/+}$ signals.

Table S4. List of genes differentially expressed in *Rac1*$^{+/-}$ and *Rac1*$^{+/+}$ mouse endothelial cells.

fold*	Gene symbol	Gene name	GB Acc.	*P*
4.24	*Cryab*	crystallin, alpha B (Cryab)	NM_009964	0.000332
3.97	*Artn*	artemin (Artn)	NM_009711	0.001038
3.11	*Psg25*	pregnancy-specific glycoprotein 25	Y13560	0.046378
3.01	*Gtf2ird1*	general transcription factor II I repeat domain-containing 1	AF289667	0.018814
2.88	*Rit2*	Ras-like without CAAX 2	NM_019692	0.01819
2.86	*Gpx3*	glutathione peroxidase 3	AK002219	0.001003
2.85	*Dsc3*	desmocollin 3	AJ000329	0.005641
2.84	*V1rd16*	vomeronasal 1 receptor, D16	AY065495	0.018947
2.80	*Slc9a2*	solute carrier family 9 (sodium/hydrogen exchanger), member 2	AF139193	0.011679
2.78	*Tff2*	trefoil factor 2 (spasmolytic protein 1) (Tff2)	NM_009363	0.012199
2.73	*Fgf5*	fibroblast growth factor 5	AB016516	0.017987
2.71	*Gpx3*	glutathione peroxidase 3 (Gpx3)	NM_008161	2.61E-05
2.67	*Glra4*	glycine receptor, alpha 4 subunit	X75853	0.024152
2.66	*2310021H06Rik*	RIKEN cDNA 2310021H06 gene	AK010143	0.047529
2.62	Med8	mediator of RNA polymerase II transcription, subunit 8 homolog (yeast)	NM_020000	0.040269
2.59	*Csh2*	chorionic somatomammotropin hormone 2	M85066	0.032345
2.57	*Ivl*	involucrin (Ivl) gene, Ivl-A6 allele, partial cds	AF290956	0.021313
2.54		Mouse DNA sequence from clone RP23-401L17 on chromosome 2, complete sequence	AL450341	0.010606
2.37	*Zkscan1*	zinc finger with KRAB and SCAN domains 1	BC016213	0.003181
2.36	*H2-D1*	histocompatibility 2, D region locus 1	M69069	0.002122
2.33	*Npas3*	neuronal PAS domain protein 3 (Npas3)	NM_013780	0.01524
2.30	*D11Ertd636e*	DNA segment, Chr 11, ERATO Doi 636, expressed	BC016190	0.016737
2.30	*Pfkfb2*	6-phosphofructo-2-kinase/fructose-2,6-biphosphatase 2 (Pfkfb2)	NM_008825	0.016121
2.28	*V2r8*	vomeronasal 2, receptor, 8 (V2r8)	NM_009494	0.030659
2.24	*V1rg4*	vomeronasal 1 receptor, G4	AY065519	0.022118
2.20	*Il7r*	interleukin 7 receptor (Il7r)	NM_008372	0.04084
2.19	*Pla2g5*	phospholipase A2, group V (Pla2g5)	NM_011110	0.011734
2.19	*1700019I23Rik*	RIKEN cDNA 1700019I23 gene (1700019I23Rik)	NM_025496	0.033292
2.18	*Olfr122*	olfactory receptor 122	AY073805	0.01079
2.18	*Pcdh10*	protocadherin 10	AF334801	0.010364
2.15	*Cst8*	cystatin 8 (cystatin-related epididymal spermatogenic)	S49926	0.022103
2.14	*Mup5*	major urinary protein 5	M16360	0.001326
2.10	*Kif9*	kinesin family member 9	AB001437	0.025084
2.09	*Oprl*	opioid receptor-like	AF043278	0.039624
2.09	*Olfr1410*	olfactory receptor 1410	AY073606	0.038755
2.08	*Olfr643*	olfactory receptor 643	AY073009	0.005425

Table S4 (continued)

2.08	*Olfr107*	olfactory receptor 107	AL133159	0.032146
2.05	*AW319487*	expressed sequence AW319487 (AW319487)	NM_054085	0.041242
2.05	*Rcn3*	reticulocalbin 3, EF-hand calcium binding domain	BC005487	0.002578
2.03	*Lsr*	lipolysis stimulated lipoprotein receptor	BC004672	0.003807
2.03	*Tcrb-V13*	T-cell receptor beta, variable 13	X00619	0.043073
2.03	*Olfr1223*	olfactory receptor 1223	AY073196	0.01518
2.03		mRNA for T-cell receptor alpha chain V region	X02932	0.008105
2.02	*2010315L10Rik*	RIKEN cDNA 2010315L10 gene	AK008573	0.004835
2.02	*Klra16*	killer cell lectin-like receptor, subfamily A, member 16 (Klra16)	NM_013794	0.00055
2.01	*Crhr2*	corticotropin releasing hormone receptor 2 (Crhr2)	NM_009953	0.023121
2.01	*Sprrl7*	small proline rich-like 7 (Sprrl7)	NM_027137	0.038317
2.00	*Smr2*	submaxillary gland androgen regulated protein 2 (Smr2)	NM_021289	0.040433
1.96	*Atp1b1*	ATPase, Na+/K+ transporting, beta 1 polypeptide (Atp1b1)	NM_009721	0.008194
1.95	*Crlf1*	cytokine receptor-like factor 1 (Crlf1)	NM_018827	0.000414
1.94	*Zdhhc12*	zinc finger, DHHC domain containing 12 (Zdhhc12)	NM_025428	0.002244
1.93	*Cxcl2*	chemokine (C-X-C motif) ligand 2 (Cxcl2)	NM_009140	0.012912
1.93	*Car8*	carbonic anhydrase 8	BC010773	0.014577
1.93	*Stra13*	stimulated by retinoic acid 13	U95003	0.038426
1.92	*1810049H19Rik*	RIKEN cDNA 1810049H19 gene	AB017031	0.039356
1.92	*5830433M19Rik*	RIKEN cDNA 5830433M19 gene	AK015743	0.045047
1.91	*Fgf14*	fibroblast growth factor 14 (Fgf14), transcript variant 1	NM_010201	0.007954
1.90	*Pscdbp*	pleckstrin homology, Sec7 and coiled-coil domains, binding protein	BC007144	0.005315
1.88	*V1rh14*	vomeronasal 1 receptor, H14	AY065540	0.039798
1.86	*Bcat1*	branched chain aminotransferase 1, cytosolic (Bcat1)	NM_007532	0.028882
1.85			AF264006	0.00682
1.85	*Dnase1*	deoxyribonuclease I (Dnase1)	NM_010061	0.021421
1.85	*Pak3*	p21 (CDKN1A)-activated kinase 3 (Pak3)	NM_008778	0.04681
1.84		Sequence 37 from Patent WO9506067	A43171	0.00041
1.84	*Kcnj5*	potassium inwardly-rectifying channel, subfamily J, member 5 (Kcnj5)	NM_010605	0.034095
1.84	*Taf9*	TAF9 RNA polymerase II, TATA box binding protein (TBP)-associated factor (Taf9)	NM_027139	0.0382
1.83	*Colec12*	collectin sub-family member 12 (Colec12)	NM_130449	0.029472
1.83	*Prr3*	proline-rich polypeptide 3	BC016636	0.012248
1.82	*Bmp6*	bone morphogenetic protein 6	J04566	0.015268
1.81	*Mybpc3*	myosin binding protein C, cardiac	AF097333	0.043749
1.81	*1810008K03Rik*	RIKEN cDNA 1810008K03 gene	AK007378	0.009176
1.81	*Mras*	muscle and microspikes RAS (Mras)	NM_008624	0.006849
1.79	*Zfp521*	zinc finger protein 521	BC021376	0.03902
1.79	*Rad52*	RAD52 homolog (S. cerevisiae)	BC019123	0.012621
1.78	*Phgdh*	3-phosphoglycerate dehydrogenase	L21027	0.022344

Table S4 (continued)

1.76	*Enpp2*	ectonucleotide pyrophosphatase/phosphodiesterase 2 (Enpp2)	NM_015744	0.022754
1.74	*Fprl1*	formyl peptide receptor-like 1 (Fprl1)	NM_008042	0.025266
1.74	*4921532D01Rik*	RIKEN cDNA 4921532D01 gene	AK014993	0.007409
1.74	*Gprc2a-rs2*	G protein-coupled receptor, family C, group 2, member A, related sequence 2	AF022251	0.048919
1.74	*Ctla2a*	cytotoxic T lymphocyte-associated protein 2 alpha (Ctla2a)	NM_007796	0.000211
1.74	*Col2a1*	procollagen, type II, alpha 1	M65161	0.018688
1.72	*Aldoa*	aldolase 1, A isoform	J05517	0.005196
1.71	*Zfp467*	zinc finger protein 467 (Zfp467)	NM_020589	0.030821
1.70	*Slc16a7*	solute carrier family 16 (monocarboxylic acid transporters), member 7 (Slc16a7)	NM_011391	0.025261
1.70	*Cxcr4*	chemokine (C-X-C motif) receptor 4	Z80112	0.001219
1.70	*Fn1*	fibronectin 1	BC004724	1.22E-05
1.69	*Fancc*	Fanconi anemia, complementation group C (Fancc)	NM_007985	0.031796
1.69	*Olfr518*	olfactory receptor 518	AY073787	0.044142
1.69	*Olfr474*	olfactory receptor 474	AY073602	0.037996
1.69	*Npy*	neuropeptide Y (Npy)	NM_023456	0.029817
1.68	*Tgfa*	transforming growth factor alpha (Tgfa)	NM_031199	0.008838
1.68	*Prph1*	peripherin 1 (Prph1)	NM_013639	0.049912
1.68	*Hspb1*	heat shock protein 1	AF047378	0.010016
1.68	*Thbs2*	thrombospondin 2 (Thbs2)	NM_011581	0.00272
1.68	*Sec6*	Sec6 protein (Sec6) gene, partial cds	AF241783	0.024738
1.67	*Akr1b8*	aldo-keto reductase family 1, member B8 (Akr1b8)	NM_008012	0.008479
1.67	*Car8*	carbonic anhydrase 8	X61397	0.002296
1.67	*Gria3*	glutamate receptor, ionotropic, AMPA3 (alpha 3) (Gria3)	NM_016886	0.040191
1.66		hypothetical protein (evidence: ORF Finder) putative; adult male testis cDNA, RIKEN full-length enriched library, clone:1700012K20 product:hypothetical protein, full insert sequence	AK005920	0.028272
1.66	*9430028I06Rik*	RIKEN cDNA 9430028I06 gene	AK008119	0.008397
1.66	*Spock1*	sparc/osteonectin, cwcv and kazal-like domains proteoglycan 1 (Spock1)	NM_009262	0.00621
1.64	*Fn1*	fibronectin 1	AF095690	0.008589
1.63	*Adcy7*	adenylate cyclase 7 (Adcy7)	NM_007406	0.00943
1.62	*Bche*	butyrylcholinesterase (Bche)	NM_009738	0.031361
1.62	*Hspa1a*	heat shock protein 1A	M12571	0.012045
1.62	*Rab5c*	RAB5C, member RAS oncogene family	BC023027	0.013248
1.62	*AI481716*	expressed sequence AI481716	BC017623	0.01596
1.61	*Tacstd2*	tumor-associated calcium signal transducer 2 (Tacstd2)	NM_020047	0.001573
1.60	*Pogz*	pogo transposable element with ZNF domain	BC014284	0.015819
1.59	*Amy2*	amylase 2, pancreatic (Amy2)	NM_009669	0.032982
1.58	*Robo4*	roundabout homolog 4 (Drosophila)	AK004723	0.010715
1.58	*Uchl1*	ubiquitin carboxy-terminal hydrolase L1 (Uchl1)	NM_011670	0.031138

Table S4 (continued)

1.57	*Klra17*	killer cell lectin-like receptor, subfamily A, member 17	AB033769	0.045451
1.57	*Tle4*	transducin-like enhancer of split 4, homolog of Drosophila E(spl)	NM_019714	0.023371
1.56	*ORF28*	open reading frame 28	BC020175	0.030425
1.56	*Cxcr4*	chemokine (C-X-C motif) receptor 4 (Cxcr4)	NM_009911	0.009266
1.55		Sequence 31 from Patent WO0177169	AX278368	0.049348
1.55	*Frs3*	fibroblast growth factor receptor substrate 3	BC014819	0.000137
1.55	*2810442O16Rik*	RIKEN cDNA 2810442O16 gene	AK006877	0.000121
1.55	*Plvap*	plasmalemma vesicle associated protein (Plvap)	NM_032398	0.000432
1.55	*Ltbp1*	latent transforming growth factor beta binding protein 1	AF280604	0.020966
1.54	*Sema7a*	sema domain, immunoglobulin domain (Ig), and GPI membrane anchor, (semaphorin) 7A (Sema7a)	NM_011352	0.008221
1.54	*Akt3*	thymoma viral proto-oncogene 3 (Akt3)	NM_011785	0.016741
1.54	*Edn1*	endothelin 1 (Edn1)	NM_010104	0.025587
1.53	*Nts*	neurotensin (Nts)	NM_024435	0.007204
1.53			NM_027343	0.008598
1.53	*Col8a1*	procollagen, type VIII, alpha 1	BC011061	0.006713
1.52	*Iars*	isoleucine-tRNA synthetase	BC002239	0.026109
1.52	*Alcam*	activated leukocyte cell adhesion molecule	L25274	0.02254
1.52	*Adamts1*	a disintegrin-like and metalloprotease (reprolysin type) with thrombospondin type 1 motif, 1 (Adamts1)	NM_009621	0.016261
1.52	*Ak1*	adenylate kinase 1 (Ak1)	NM_021515	0.045794
1.52	*Cacnb3*	calcium channel, voltage-dependent, beta 3 subunit (Cacnb3)	NM_007581	0.008666
1.52	*Spp1*	secreted phosphoprotein 1 (Spp1)	NM_009263	0.004518
1.51	*Mrrf*	mitochondrial ribosome recycling factor	AK010018	0.005785
1.50	*Olfr2*	olfactory receptor 2	AF178751	0.029528
1.50	*Atf5*	activating transcription factor 5 (Atf5)	NM_030693	0.009712
-1.51	*Hmgb2*	high mobility group box 2	X67668	0.029193
-1.51	*2810406K13Rik*	RIKEN cDNA 2810406K13 gene	AK013012	0.034717
-1.51	*Prim1*	DNA primase, p49 subunit (Prim1)	NM_008921	0.028811
-1.52	*Cacng4*	calcium channel, voltage-dependent, gamma subunit 4 (Cacng4)	NM_019431	0.041871
-1.52	*Sn*	sialoadhesin (Sn)	NM_011426	0.036618
-1.52	*Hist2h2aa1*	histone 2, H2aa1	Z30940	0.005384
-1.52	*Hmgb2*	high mobility group box 2	NM_008252	0.007386
-1.52	*Hist1h2ai*	histone 1, H2ai	X05862	0.000777
-1.52	*Ang1*	angiogenin, ribonuclease A family, member 1 (Ang1)	NM_007447	0.008404
-1.53	*Cldn15*	claudin 15 (Cldn15)	NM_021719	0.009868
-1.53	*2610109H07Rik*	RIKEN cDNA 2610109H07 gene	AK011831	0.042316
-1.54	*Fah*	fumarylacetoacetate hydrolase (Fah)	NM_010176	0.032904
-1.54	*4933413J09Rik*	RIKEN cDNA 4933413J09 gene	AK016807	0.008573
-1.54	*Nrp2*	neuropilin 2	AF022858	0.010839
-1.54	*Mcm10*	minichromosome maintenance deficient 10 (S. cerevisiae)	AK021211	0.035852

Table S4 (continued)

-1.54	*Cdca5*	Cell division cycle associated 5	NM_026410	0.027833
-1.55	*Pax7*	paired box gene 7	AF254422	0.035047
-1.55	*Racgap1*	Rac GTPase-activating protein 1 (Racgap1)	NM_012025	0.001656
-1.56	*Ki-67*	mRNA fragment for Ki-67 antigen	X94763	0.017855
-1.56	*CRG-L1*	cancer related gene-liver 1	AF282864	0.002256
-1.57	*Pmf1*	polyamine-modulated factor 1 (Pmf1)	NM_025928	0.002309
-1.57	*Hist1h2ab*	histone 1, H2ab	M37736	0.010863
-1.57	*Mcam*	melanoma cell adhesion molecule (Mcam)	NM_023061	0.006146
-1.57	*2310057H16Rik*	RIKEN cDNA 2310057H16 gene	BC008225	8.91E-05
-1.57	*Myb*	myeloblastosis oncogene	X02774	0.002447
-1.57		0 day neonate skin cDNA, RIKEN full-length enriched library, clone:4632427M03 product:coatomer protein complex, subunit gamma 1, full insert sequence	AK014595	0.0271
-1.57	*Hist1h2ab*	histone 1, H2ab	M33988	0.007678
-1.57	*Bard1*	BRCA1 associated RING domain 1 (Bard1)	NM_007525	0.017774
-1.58	*1700027M21Rik*	RIKEN cDNA 1700027M21 gene	AK007194	0.041362
-1.58	*Donson*	downstream neighbor of SON	AF193608	0.002667
-1.58	*Kif22*	kinesin family member 22	BC003427	0.002712
-1.58	*Agpat2*	1- acylglycerol-3-phosphate O-acyltransferase 2 (lysophosphatidic acid acyltransferase, beta)	AK002422	0.026779
-1.58	*Rab3c*	RAB3C, member RAS oncogene family	AK012468	0.00092
-1.58	*Pfn3*	profilin 3	AK005930	0.015965
-1.58	*Mapt*	microtubule-associated protein tau	M18775	0.007396
-1.58	*Gpr12*	G-protein coupled receptor 12 (Gpr12)	NM_008151	0.015134
-1.59	*Kif23*	kinesin family member 23 (Kif23)	NM_024245	0.041941
-1.59	*Ccna2*	cyclin A2 (Ccna2)	NM_009828	0.002881
-1.59	*Birc5*	baculoviral IAP repeat-containing 5	AF115517	0.028478
-1.60	*1110003P22Rik*	RIKEN cDNA 1110003P22 gene	AF285112	0.006315
-1.60	*Biklk*	Bcl2-interacting killer-like	BC003732	0.028602
-1.60	*Mad2l1*	MAD2 (mitotic arrest deficient, homolog)-like 1 (yeast) (Mad2l1)	NM_019499	0.03936
-1.61	*Npl*	N-acetylneuraminate pyruvate lyase	AK002734	0.042953
-1.61	*Mapk8ip3*	mitogen-activated protein kinase 8 interacting protein 3 (Mapk8ip3)	NM_013931	0.002131
-1.61	*Card14*	caspase recruitment domain family, member 14	BC004692	0.032207
-1.62	*Prc1*	protein regulator of cytokinesis 1	AF408435	0.029025
-1.62	*Biklk*	Bcl2-interacting killer-like (Biklk)	NM_007546	0.012093
-1.62	*Txnrd1*	thioredoxin reductase 1	AF333036	0.018651
-1.62	*Tacc3*	transforming, acidic coiled-coil containing protein 3	AF247674	0.006697
-1.63	*Anln*	anillin, actin binding protein (scraps homolog, Drosophila)	AK013624	0.007416
-1.64	*Stk6*	serine/threonine kinase 6	AF007817	0.010775
-1.64	*Prss15*	protease, serine, 15	AK004820	0.000708
-1.64	*8430417G17Rik*	RIKEN cDNA 8430417G17 gene	AK018423	0.011151

Table S4 (continued)

-1.64	*Aqp8*	aquaporin 8	BC010982	0.005582
-1.64	*A030007L17Rik*	RIKEN cDNA A030007L17 gene	AK008719	0.005629
-1.65	*Htr6*	5-hydroxytryptamine (serotonin) receptor 6 (Htr6)	NM_021358	0.022271
-1.65	*Ect2*	ect2 oncogene (Ect2)	NM_007900	0.000159
-1.65	*Nrp2*	neuropilin 2	AF022854	0.001666
-1.65	*Kif2c*	kinesin family member 2C	BC006841	0.047132
-1.65	*Nrp2*	neuropilin 2	AF022856	0.041525
-1.65	*Nrp2*	neuropilin 2	AF022861	0.001322
-1.66	*4121402D02Rik*	RIKEN cDNA 4121402D02 gene	AK015496	0.038647
-1.66	*Hmmr*	hyaluronan mediated motility receptor (RHAMM)	X64550	0.003415
-1.66	*Tk1*	thymidine kinase 1 (Tk1)	NM_009387	0.01588
-1.66	*Cdca3*	cell division cycle associated 3 (Cdca3)	NM_013538	0.009774
-1.66	*Bmx*	BMX non-receptor tyrosine kinase (Bmx)	NM_009759	0.001709
-1.67	*Hist2h2ac*	histone 2, H2ac	U62673	0.034253
-1.67	*Ryr3*	ryanodine receptor 3	AF111166	0.046717
-1.67	*Gadd45g*	growth arrest and DNA-damage-inducible 45 gamma	AK007410	0.000456
-1.68	*BC004701*	cDNA sequence BC004701	BC004701	0.004271
-1.68	*Chc1l*	chromosome condensation 1-like	BC003224	0.037379
-1.68	*Gpr83*	G protein-coupled receptor 83	Y19227	0.014326
-1.68	*Olfr900*	olfactory receptor 900	AY073216	0.00421
-1.68	*2810418N01Rik*	RIKEN cDNA 2810418N01 gene	AK013116	0.0005
-1.69	*Scrn1*	secernin 1	AK012765	0.019703
-1.70	*2600013E07Rik*	RIKEN cDNA 2600013E07 gene	AK011195	0.030419
-1.70	*Cdca1*	cell division cycle associated 1 (Cdca1)	NM_023284	0.012767
-1.70	*2300006N05Rik*	RIKEN cDNA 2300006N05 gene (2300006N05Rik)	NM_027087	0.011339
-1.70	*Gadd45g*	growth arrest and DNA-damage-inducible 45 gamma (Gadd45g)	NM_011817	0.004336
-1.71	*Fignl1*	fidgetin-like 1 (Fignl1)	NM_021891	0.007444
-1.71	*1700023B02Rik*	RIKEN cDNA 1700023B02 gene (1700023B02Rik)	NM_025854	0.002954
-1.71	*Shcbp1*	Shc SH2-domain binding protein 1 (Shcbp1)	NM_011369	0.028062
-1.71	*Zfp69*	zinc finger protein 69	U29497	0.012597
-1.72	*Nos2*	nitric oxide synthase 2, inducible, macrophage (Nos2)	NM_010927	0.015464
-1.72	*Troap*	trophinin associated protein	AK021408	0.001501
-1.72	*4933434L15Rik*	RIKEN cDNA 4933434L15 gene	AK020021	0.005267
-1.73	*Elavl3*	ELAV (embryonic lethal, abnormal vision, Drosophila)-like 3 (Hu antigen C)	U29148	0.01646
-1.73	*Runx1*	runt related transcription factor 1	D13802	0.016366
-1.73	*Kif20b*	kinesin family member 20B	AB054030	0.037964
-1.73	*Hist2h2bb*	histone 2, H2bb	U62675	0.002737
-1.74	*Hist1h2bb*	histone 1, H2bb	X80328	0.002342
-1.74	*Kif18a*	kinesin family member 18A	BC016095	0.030763
-1.74	*Aqp8*	aquaporin 8	AF084531	0.003986

Table S4 (continued)

-1.75	*Tpx2*	TPX2, microtubule-associated protein homolog (Xenopus laevis)	AK011311	0.001425
-1.75	*Cdkn2c*	cyclin-dependent kinase inhibitor 2C (p18, inhibits CDK4) (Cdkn2c)	NM_007671	0.013
-1.76	*Kif20a*	kinesin family member 20A (Kif20a)	NM_009004	0.012885
-1.77	*Nrp2*	neuropilin 2	AF022857	0.000154
-1.77	*Hist1h1a*	histone 1, H1a	Y12290	0.010093
-1.78	*Prc1*	protein regulator of cytokinesis 1	BC005475	0.034846
-1.78	*Rnase4*	ribonuclease, RNase A family 4 (Rnase4), transcript variant 1	NM_021472	0.003887
-1.78	*Aqp8*	aquaporin 8 (Aqp8)	NM_007474	0.005305
-1.79	*3200002M19Rik*	RIKEN cDNA 3200002M19 gene	AK018169	0.016628
-1.79	*Ifit2*	interferon-induced protein with tetratricopeptide repeats 2 (Ifit2)	NM_008332	0.000455
-1.80	*H2-Eb2*	histocompatibility 2, class II antigen E beta2	X04437	0.003988
-1.80	*Cenpe*	centromere protein E	AB001426	4.85E-05
-1.80	*2900070E19Rik*	RIKEN cDNA 2900070E19 gene	AK013761	0.001642
-1.80	*Tacc3*	transforming, acidic coiled-coil containing protein 3	AF203445	0.000815
-1.81	*Sil*	Tal1 interrupting locus (Sil)	NM_009185	0.001899
-1.82	*Hist1h3f*	histone 1, H3f	X01685	0.003797
-1.82	*Ms4a6b*	membrane-spanning 4-domains, subfamily A, member 6B (Ms4a6b)	NM_027209	0.005783
-1.82	*Tacc3*	transforming, acidic coiled-coil containing protein 3 (Tacc3)	NM_011524	0.015851
-1.82	*Rragd*	Ras-related GTP binding D	AK017818	0.001269
-1.82	*Bsn*	bassoon	AK010775	0.00223
-1.83	*Hist1h3f*	histone 1, H3f (Hist1h3f)	NM_013548	0.007657
-1.85	*Nek2*	NIMA (never in mitosis gene a)-related expressed kinase 2 (Nek2)	NM_010892	0.030419
-1.86	*Gpr83*	G protein-coupled receptor 83 (Gpr83)	NM_010287	0.000598
-1.87	*Top2a*	topoisomerase (DNA) II alpha (Top2a)	NM_011623	0.000408
-1.87	*Hsd17b7*	hydroxysteroid (17-beta) dehydrogenase 7 (Hsd17b7)	NM_010476	0.012615
-1.88	*Ctsk*	cathepsin K (Ctsk)	NM_007802	0.014425
-1.88	*Ccnb2*	cyclin B2 (Ccnb2)	NM_007630	0.002149
-1.88	*Ccl2*	chemokine (C-C motif) ligand 2 (Ccl2)	NM_011333	0.043278
-1.88		histone H2A (AA 1-130); Murine H2A gene for histone H2A	X16495	0.002229
-1.90	*Birc5*	baculoviral IAP repeat-containing 5	AF115517	0.002143
-1.93	*Tacc3*	transforming, acidic coiled-coil containing protein 3	BC003252	0.005181
-1.94	*Slc7a10*	solute carrier family 7 (cationic amino acid transporter, y+ system), member 10 (Slc7a10)	NM_017394	0.001133
-1.94	*Hist1h3g*	histone 1, H3g	X16496	0.009319
-1.95	*Ryr3*	ryanodine receptor 3	U23756	0.021424
-1.96	*6720460F02Rik*	RIKEN cDNA 6720460F02 gene	BC020115	0.021213
-1.96	*Serpina3n*	serine (or cysteine) proteinase inhibitor, clade A, member 3N (Serpina3n)	NM_009252	0.000104
-1.96	*Col14a1*	procollagen, type XIV, alpha 1	AJ131395	0.021011
-1.97	*4930431B09Rik*	RIKEN cDNA 4930431B09 gene	AK015259	0.00142

Table S4 (continued)

-1.97	*Diap3*	diaphanous homolog 3 (Drosophila) (Diap3)	NM_019670	0.017345
-1.97	*Foxj2*	forkhead box J2 (Foxj2)	NM_021899	0.043415
-1.99	*Has1*	hyaluronan synthase1 (Has1)	NM_008215	0.010534
-1.99	*Hist1h1b*	histone 1, H1b	Z46227	0.00303
-2.01	*Col6a3*	procollagen, type VI, alpha 3	AF034136	0.045159
-2.04	*Mapt*	microtubule-associated protein tau	U12916	0.014972
-2.04	*Cd97*	CD97 antigen (Cd97)	NM_011925	0.045557
-2.04	*Melk*	maternal embryonic leucine zipper kinase (Melk)	NM_010790	0.030684
-2.05	*4930427A07Rik*	RIKEN cDNA 4930427A07 gene	BC022617	0.01435
-2.05	*Kif11*	kinesin family member 11	AJ223293	0.000144
-2.06		cyclinA gene, partial cds	U57826	0.001726
-2.06	*Mapt*	microtubule-associated protein tau	M18776	0.005166
-2.06	*Cdkn3*	cyclin-dependent kinase inhibitor 3	AK010426	0.025191
-2.09	*6330411I15Rik*	RIKEN cDNA 6330411I15 gene	AK018160	0.040013
-2.11	*Cdc2a*	cell division cycle 2 homolog A (S. pombe) (Cdc2a)	NM_007659	0.003414
-2.12	*Pbk*	PDZ binding kinase (Pbk)	NM_023209	0.001764
-2.18	*Cenpf*	centromere autoantigen F	AF194970	0.03014
-2.20	*Plxnc1*	plexin C1 (Plxnc1)	NM_018797	0.024925
-2.23	*Mki67*	antigen identified by monoclonal antibody Ki 67	X82786	0.000242
-2.26	*Trim6*	tripartite motif protein 6	AF220031	0.039421
-2.29	*Anxa8*	annexin A8	BC013271	0.001791
-2.29	*4930441F12Rik*	RIKEN cDNA 4930441F12 gene	AK019605	0.049089
-2.36			NM_014195	0.02471
-2.46	*Egr1*	early growth response 1 (Egr1)	NM_007913	0.001094
-2.49	*4930488P06Rik*	RIKEN cDNA 4930488P06 gene	BC003258	0.002046
-2.83	*Ccl21b*	chemokine (C-C motif) ligand 21b (serine) (Ccl21b)	NM_011124	0.002242
-3.02	*Fos*	FBJ osteosarcoma oncogene (Fos)	NM_010234	0.000701
-3.15	*Pla2g2f*	phospholipase A2, group IIF (Pla2g2f)	NM_012045	6.08E-05
-3.28	*Fgl2*	fibrinogen-like protein 2 (Fgl2)	NM_008013	0.014771
-4.11	*Ugt1a6*	UDP glycosyltransferase 1 family, polypeptide A6	D87867	0.016287

* The fold ratio of *Rac1*$^{+/-}$/*Rac1*$^{+/+}$ signals.

Supplementary References and Notes

1. M. Glogauer, C. C. Marchal, F. Zhu, A. Worku, B. E. Clausen, I. Foerster, P. Marks, G. P. Downey, M. Dinauer, D. J. Kwiatkowski, Rac1 deletion in mouse neutrophils has selective effects on neutrophil functions. *J Immunol* **170**, 5652-5657 (2003).
2. P. A. Koni, S. K. Joshi, U. A. Temann, D. Olson, L. Burkly, R. A. Flavell, Conditional vascular cell adhesion molecule 1 deletion in mice: impaired lymphocyte migration to bone marrow. *J Exp Med* **193**, 741-754 (2001).
3. H. H. Kim, N. Sawada, G. Soydan, H. S. Lee, Z. Zhou, S. K. Hwang, C. Waeber, M. A. Moskowitz, J. K. Liao, Additive effects of statin and dipyridamole on cerebral blood flow and stroke protection. *J Cereb Blood Flow Metab*, (2008).
4. Y. C. Lim, G. Garcia-Cardena, J. R. Allport, M. Zervoglos, A. J. Connolly, M. A. Gimbrone, Jr., F. W. Luscinskas, Heterogeneity of endothelial cells from different organ sites in T-cell subset recruitment. *Am J Pathol* **162**, 1591-1601 (2003).
5. E. E. Sander, S. van Delft, J. P. ten Klooster, T. Reid, R. A. van der Kammen, F. Michiels, J. G. Collard, Matrix-dependent Tiam1/Rac signaling in epithelial cells promotes either cell-cell adhesion or cell migration and is regulated by phosphatidylinositol 3-kinase. *J Cell Biol* **143**, 1385-1398 (1998).
6. G. Dennis, Jr., B. T. Sherman, D. A. Hosack, J. Yang, W. Gao, H. C. Lane, R. A. Lempicki, DAVID: Database for Annotation, Visualization, and Integrated Discovery. *Genome Biol* **4**, P3 (2003).
7. A. Subramanian, P. Tamayo, V. K. Mootha, S. Mukherjee, B. L. Ebert, M. A. Gillette, A. Paulovich, S. L. Pomeroy, T. R. Golub, E. S. Lander, J. P. Mesirov, Gene set enrichment analysis: a knowledge-based approach for interpreting genome-wide expression profiles. *Proc Natl Acad Sci U S A* **102**, 15545-15550 (2005).
8. M. P. Quinlan, Rac regulates the stability of the adherens junction and its components, thus affecting epithelial cell differentiation and transformation. *Oncogene* **18**, 6434-6442 (1999).
9. R. A. Stockton, E. Schaefer, M. A. Schwartz, p21-activated kinase regulates endothelial permeability through modulation of contractility. *J Biol Chem* **279**, 46621-46630 (2004).
10. H. Gao, M. Liang, A. Bergdahl, A. Hamren, M. W. Lindholm, K. Dahlman-Wright, B. O. Nilsson, Estrogen attenuates vascular expression of inflammation associated genes and adhesion of monocytes to endothelial cells. *Inflamm Res* **55**, 349-353 (2006).
11. Z. Wu, F. M. Hofman, B. V. Zlokovic, A simple method for isolation and characterization of mouse brain microvascular endothelial cells. *J Neurosci Methods* **130**, 53-63 (2003).
12. L. Song, J. S. Pachter, Culture of murine brain microvascular endothelial cells that maintain expression and cytoskeletal association of tight junction-associated proteins. *In Vitro Cell Dev Biol Anim* **39**, 313-320 (2003).
13. C. Weidenfeller, S. Schrot, A. Zozulya, H. J. Galla, Murine brain capillary endothelial cells exhibit improved barrier properties under the influence of hydrocortisone. *Brain Res* **1053**, 162-174 (2005).
14. S. Orsulic, Y. Li, R. A. Soslow, L. A. Vitale-Cross, J. S. Gutkind, H. E. Varmus, Induction of ovarian cancer by defined multiple genetic changes in a mouse model system. *Cancer Cell* **1**, 53-62 (2002).
15. J. R. Brown, E. Nigh, R. J. Lee, H. Ye, M. A. Thompson, F. Saudou, R. G. Pestell, M. E. Greenberg, Fos family members induce cell cycle entry by activating cyclin D1. *Mol Cell Biol* **18**, 5609-5619 (1998).
16. Y. Nakata, S. Shetzline, C. Sakashita, A. Kalota, R. Rallapalli, S. I. Rudnick, Y. Zhang, S. G. Emerson, A. M. Gewirtz, c-Myb contributes to G2/M cell cycle transition in human hematopoietic cells by direct regulation of cyclin B1 expression. *Mol Cell Biol* **27**, 2048-2058 (2007).
17. V. P. Sukhatme, Early transcriptional events in cell growth: the Egr family. *J Am Soc Nephrol* **1**, 859-866 (1990).
18. F. Bernardin, A. D. Friedman, AML1 stimulates G1 to S progression via its transactivation domain. *Oncogene* **21**, 3247-3252 (2002).
19. T. Hirota, N. Kunitoku, T. Sasayama, T. Marumoto, D. Zhang, M. Nitta, K. Hatakeyama, H. Saya,

Aurora-A and an interacting activator, the LIM protein Ajuba, are required for mitotic commitment in human cells. *Cell* **114**, 585-598 (2003).

20. L. Schneider, F. Essmann, A. Kletke, P. Rio, H. Hanenberg, W. Wetzel, K. Schulze-Osthoff, B. Nurnberg, R. P. Piekorz, The transforming acidic coiled coil 3 protein is essential for spindle-dependent chromosome alignment and mitotic survival. *J Biol Chem* **282**, 29273-29283 (2007).
21. R. Bayliss, T. Sardon, I. Vernos, E. Conti, Structural basis of Aurora-A activation by TPX2 at the mitotic spindle. *Mol Cell* **12**, 851-862 (2003).
22. V. Joukov, A. C. Groen, T. Prokhorova, R. Gerson, E. White, A. Rodriguez, J. C. Walter, D. M. Livingston, The BRCA1/BARD1 heterodimer modulates ran-dependent mitotic spindle assembly. *Cell* **127**, 539-552 (2006).
23. G. Fang, H. Yu, M. W. Kirschner, The checkpoint protein MAD2 and the mitotic regulator CDC20 form a ternary complex with the anaphase-promoting complex to control anaphase initiation. *Genes Dev* **12**, 1871-1883 (1998).
24. A. Giodini, M. J. Kallio, N. R. Wall, G. J. Gorbsky, S. Tognin, P. C. Marchisio, M. Symons, D. C. Altieri, Regulation of microtubule stability and mitotic progression by survivin. *Cancer Res* **62**, 2462-2467 (2002).
25. A. M. Fry, P. Meraldi, E. A. Nigg, A centrosomal function for the human Nek2 protein kinase, a member of the NIMA family of cell cycle regulators. *EMBO J* **17**, 470-481 (1998).
26. T. Tatsumoto, X. Xie, R. Blumenthal, I. Okamoto, T. Miki, Human ECT2 is an exchange factor for Rho GTPases, phosphorylated in G2/M phases, and involved in cytokinesis. *J Cell Biol* **147**, 921-928 (1999).
27. J. Schmitz, E. Watrin, P. Lenart, K. Mechtler, J. M. Peters, Sororin is required for stable binding of cohesin to chromatin and for sister chromatid cohesion in interphase. *Curr Biol* **17**, 630-636 (2007).
28. X. W. Wang, Q. Zhan, J. D. Coursen, M. A. Khan, H. U. Kontny, L. Yu, M. C. Hollander, P. M. O'Connor, A. J. Fornace, Jr., C. C. Harris, GADD45 induction of a G2/M cell cycle checkpoint. *Proc Natl Acad Sci U S A* **96**, 3706-3711 (1999).
29. H. Miki, Y. Okada, N. Hirokawa, Analysis of the kinesin superfamily: insights into structure and function. *Trends Cell Biol* **15**, 467-476 (2005).
30. A. Blangy, H. A. Lane, P. d'Herin, M. Harper, M. Kress, E. A. Nigg, Phosphorylation by p34cdc2 regulates spindle association of human Eg5, a kinesin-related motor essential for bipolar spindle formation in vivo. *Cell* **83**, 1159-1169 (1995).
31. A. A. Levesque, D. A. Compton, The chromokinesin Kid is necessary for chromosome arm orientation and oscillation, but not congression, on mitotic spindles. *J Cell Biol* **154**, 1135-1146 (2001).
32. R. Neef, U. R. Klein, R. Kopajtich, F. A. Barr, Cooperation between mitotic kinesins controls the late stages of cytokinesis. *Curr Biol* **16**, 301-307 (2006).
33. P. D. Andrews, Y. Ovechkina, N. Morrice, M. Wagenbach, K. Duncan, L. Wordeman, J. R. Swedlow, Aurora B regulates MCAK at the mitotic centromere. *Dev Cell* **6**, 253-268 (2004).
34. J. Stumpff, G. von Dassow, M. Wagenbach, C. Asbury, L. Wordeman, The kinesin-8 motor Kif18A suppresses kinetochore movements to control mitotic chromosome alignment. *Dev Cell* **14**, 252-262 (2008).
35. E. Hill, M. Clarke, F. A. Barr, The Rab6-binding kinesin, Rab6-KIFL, is required for cytokinesis. *EMBO J* **19**, 5711-5719 (2000).
36. F. Bernardin-Fried, T. Kummalue, S. Leijen, M. I. Collector, K. Ravid, A. D. Friedman, AML1/RUNX1 increases during G1 to S cell cycle progression independent of cytokine-dependent phosphorylation and induces cyclin D3 gene expression. *J Biol Chem* **279**, 15678-15687 (2004).
37. S. J. Schultz, A. M. Fry, C. Sutterlin, T. Ried, E. A. Nigg, Cell cycle-dependent expression of Nek2, a novel human protein kinase related to the NIMA mitotic regulator of Aspergillus nidulans. *Cell Growth Differ* **5**, 625-635 (1994).
38. H. Sakata, J. S. Rubin, W. G. Taylor, T. Miki, A Rho-specific exchange factor Ect2 is induced from S to M phases in regenerating mouse liver. *Hepatology* **32**, 193-199 (2000).
39. M. Tanaka, A. Ueda, H. Kanamori, H. Ideguchi, J. Yang, S. Kitajima, Y. Ishigatsubo, Cell-cycle-

dependent regulation of human aurora A transcription is mediated by periodic repression of E4TF1. *J Biol Chem* **277**, 10719-10726 (2002).

40. W. F. Marzluff, R. J. Duronio, Histone mRNA expression: multiple levels of cell cycle regulation and important developmental consequences. *Curr Opin Cell Biol* **14**, 692-699 (2002).
41. K. Kimura, M. Saijo, M. Ui, T. Enomoto, Growth state- and cell cycle-dependent fluctuation in the expression of two forms of DNA topoisomerase II and possible specific modification of the higher molecular weight form in the M phase. *J Biol Chem* **269**, 1173-1176 (1994).
42. M. F. Olson, A. Ashworth, A. Hall, An essential role for Rho, Rac, and Cdc42 GTPases in cell cycle progression through G1. *Science* **269**, 1270-1272 (1995).
43. D. Michaelson, W. Abidi, D. Guardavaccaro, M. Zhou, I. Ahearn, M. Pagano, M. R. Philips, Rac1 accumulates in the nucleus during the G2 phase of the cell cycle and promotes cell division. *J Cell Biol* **181**, 485-496 (2008).
44. C. S. Hill, J. Wynne, R. Treisman, The Rho family GTPases RhoA, Rac1, and CDC42Hs regulate transcriptional activation by SRF. *Cell* **81**, 1159-1170 (1995).
45. C. A. Jones, N. R. London, H. Chen, K. W. Park, D. Sauvaget, R. A. Stockton, J. D. Wythe, W. Suh, F. Larrieu-Lahargue, Y. S. Mukouyama, P. Lindblom, P. Seth, A. Frias, N. Nishiya, M. H. Ginsberg, H. Gerhardt, K. Zhang, D. Y. Li, Robo4 stabilizes the vascular network by inhibiting pathologic angiogenesis and endothelial hyperpermeability. *Nat Med* **14**, 448-453 (2008).
46. F. Vazquez, G. Hastings, M. A. Ortega, T. F. Lane, S. Oikemus, M. Lombardo, M. L. Iruela-Arispe, METH-1, a human ortholog of ADAMTS-1, and METH-2 are members of a new family of proteins with angio-inhibitory activity. *J Biol Chem* **274**, 23349-23357 (1999).
47. B. Lange-Asschenfeldt, W. Weninger, P. Velasco, T. R. Kyriakides, U. H. von Andrian, P. Bornstein, M. Detmar, Increased and prolonged inflammation and angiogenesis in delayed-type hypersensitivity reactions elicited in the skin of thrombospondin-2--deficient mice. *Blood* **99**, 538-545 (2002).
48. N. Sawada, S. Salomone, H. H. Kim, D. J. Kwiatkowski, J. K. Liao, Regulation of endothelial nitric oxide synthase and postnatal angiogenesis by Rac1. *Circ Res* **103**, 360-368 (2008).